

Hole-density evolution of the one-particle spectral function in doped ladders

George B. Martins, Claudio Gazza, and Elbio Dagotto

National High Magnetic Field Laboratory and Department of Physics, Florida State University, Tallahassee, Florida 32306

(Received 26 February 1999)

The spectral function $A(\mathbf{q}, \omega)$ of doped t - J ladders is presented on clusters with up to 2×20 sites at zero temperature applying a recently developed technique that uses up to $\sim 6 \times 10^6$ rung-basis states. Similarities with photoemission results for the two-dimensional cuprates are observed, such as the existence of a gap at $(\pi, 0)$ near half-filling (caused by hole pair formation) and flat bands in its vicinity. These features should be observable in angle-resolved photoemission spectroscopy experiments on ladders. The main result of the paper is the nontrivial evolution of the spectral function from a narrow band at $x=0$, to a quasilinear band at $x \geq 0.5$. It was also observed that the low-energy peaks of a cluster spectra acquire finite linewidths as their energies move away from the chemical potential. [S0163-1829(99)08621-X]

Copper-oxide ladder compounds are currently under much investigation.¹ Among their interesting properties are a spin-liquid ground state in the undoped limit, and the existence of superconductivity upon hole doping.^{2,3} Recently, the first angle-resolved photoemission (ARPES) studies of ladder materials have been reported. Both the doped and undoped ladder $\text{Sr}_{14}\text{Cu}_{24}\text{O}_{41}$ have been analyzed, finding one-dimensional metallic characteristics.⁴ Studies of the ladder compound $\text{La}_{1-x}\text{Sr}_x\text{CuO}_{2.5}$ found similarities with $\text{La}_{2-x}\text{Sr}_x\text{CuO}_4$, including a Fermi edge.⁵ Core-level photoemission experiments for $(\text{La}, \text{Sr}, \text{Ca})_{14}\text{Cu}_{24}\text{O}_{41}$ documented its chemical shift against hole concentration.⁶ Note that the importance of ARPES studies for other materials such as the high- T_c cuprates is by now clearly established.⁷ Using this technique the evolution with doping of the Fermi surface has been discussed,⁸ including the existence of flat bands near momenta $(0, \pi) - (\pi, 0)$.⁹

This plethora of experimental results for the cuprates should be compared against theoretical predictions. However, the calculation of the ARPES response even for simple models is a formidable task. The most reliable computational tools for these calculations are the exact diagonalization (ED) method, restricted to small clusters, and the quantum Monte Carlo (QMC) technique supplemented by maximum entropy, limited in doped systems to high temperatures due to the sign problem. Currently, on ladders dynamical properties can be exactly calculated at all densities only on clusters of size 2×8 ,¹⁰⁻¹² while the QMC technique in the realistic regime of large U/t (Hubbard model) has been applied on 2×16 lattices only at half-filling¹³ and with one hole,¹⁴ the latter using an anisotropic ladder since for the isotropic case the sign problem is severe.

Due to the limitations of these techniques an important issue still unclear is the evolution of the one-particle spectral function between the undoped limit, dominated by antiferromagnetic (AF) fluctuations both on ladders and planes, and the high hole-density regime where those fluctuations are negligible. While both extreme cases are properly treated by previously available numerical methods, the transition from one to the other as the hole density x grows is still unknown. This evolution is expected to be highly nontrivial. For instance, the presence of hole pairs in lightly doped ladders

suggests the opening of a gap in ARPES, similar to the pseudogap of underdoped high- T_c cuprates.¹⁵ Shadow-band features in undoped ladders,¹¹ which are absent at higher hole densities, add to the complexity of this evolution.

Motivated by this challenging problem, in this paper the density evolution of the spectral function $A(\mathbf{q}, \omega)$ of doped two-leg t - J ladders is presented. The calculation is carried out at zero temperature on clusters with up to 2×20 sites, increasing by a substantial factor the current resolution of the ED techniques. These intermediate size clusters were reached by working with a small fraction of the total Hilbert space of the system.¹⁶ The method is variational, although accurate as shown below. The improvement over previous efforts lies in the procedure used to select the basis states of the problem.¹⁷ The generation of the basis is in the same spirit as any technique of the renormalization-group (RG) family. If the standard S_z basis is used (three states per site), experience shows that a large number of states is needed to reproduce qualitatively the spin-liquid characteristics of the undoped ladders. The reason is that in the S_z basis one of the states with the highest weight in the ground state is still the Néel state, in spite of the existence of a short AF correlation length ξ_{AF} . A small basis built up around the Néel state incorrectly favors long-range spin order. However, if the Hamiltonian of the problem is exactly rewritten in, e.g., the *rung* basis (9 states/rung for the t - J model) before the expansion of the Hilbert space is performed, then the tendency to favor a small ξ_{AF} is natural since one of the dominant states in this basis for the undoped case corresponds to the direct product of singlets in each rung, $|S\rangle$, which has $\xi_{\text{AF}} = 0$ along the chains. Fluctuations of the resonant-valence-bond (RVB) variety around $|S\rangle$ appear naturally in this representation of the Hamiltonian leading to a finite ξ_{AF} . Note that $|S\rangle$ is just *one* state of the rung basis, while in the S_z basis it is represented by 2^{N_r} states with N_r the number of rungs of the two-leg ladder. In general, a few states in the rung basis are equivalent to a large number of states in the S_z basis. Expanding the Hilbert space in the new representation is equivalent to working in the S_z basis with a number of states larger than can be reached directly with present day computers. Here for simplicity this technique will be referred to as the optimized reduced basis approximation (ORBA).¹⁷

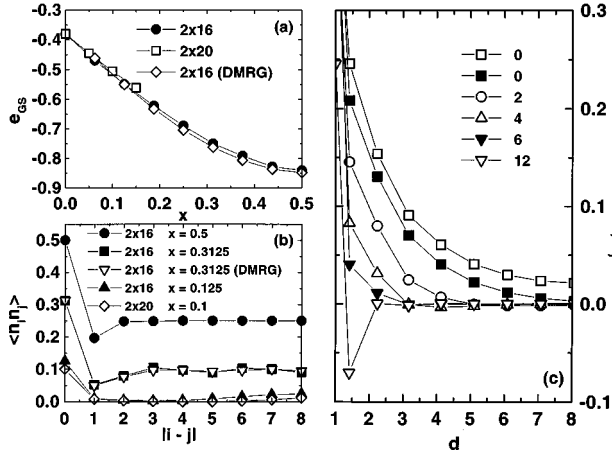


FIG. 1. (a) e_{GS} vs x for the t - J model using the method described in this paper for the two clusters indicated ($t=1$). DMRG results with OBC are also provided for comparison; (b) Ground-state hole-hole density correlations vs distance for a variety of clusters and densities as indicated; (c) Ground-state staggered spin-spin correlations vs distance d ($=|\mathbf{i}-\mathbf{j}|$) along the leg opposite to where site \mathbf{i} is located. The number of holes are indicated. Some results with DMRG are also shown. Open (full) symbols are for 2×16 (2×20) clusters.

As a first step, let us compare ORBA predictions for equal-time observables against density matrix renormalization group (DMRG) results¹⁸ for the same clusters. Here a coupling $J/t=0.4$ is used. Its particular value is important: if J/t is smaller, then pairs are lost while if it is larger superconducting correlations are important. Only in a small window of J/t can the ground state be considered as formed by weakly interacting hole pairs, a regime that we want to investigate in this paper for its possible connection with the phenomenology of high- T_c at finite temperature. Figure 1(a) contains the ground-state energy per site e_{GS} vs x using $\sim 2-3 \times 10^6$ states in the rung basis. The DMRG energies are obtained with $m=200$ states and open boundary conditions (OBC's). Both sets of data are in good agreement.¹⁹ On 2×20 clusters, the rung-basis approach allowed us to study up to six holes,²⁰ which has a full space of $\sim 10^{14}$ states (for zero momentum and total spin), while the largest previously reported exact study on a 2×10 cluster and two holes needs a $\sim 5 \times 10^5$ basis.^{10,11} Calculating the binding energy, or the chemical potential μ vs x , from e_{GS} supplemented by the energies for an odd number of electrons, a tendency to pair formation at low hole-density was observed.^{10,21} Figure 1(b) contains the hole-hole correlations at several densities, compared (in one case) with DMRG results. In Fig. 1(c) spin-spin correlations are shown. The rung-basis properly reproduces the existence of a small ξ_{AF} in the ground state, that decreases as x grows. This technique captures the essence of the ground-state behavior.

To produce dynamical results Ref. 17 was followed, namely $\sim 10-20\%$ states of the reduced basis N -holes ground state $|\psi_0\rangle$ were considered²² and the reduced subspace with, e.g., $N+1$ holes and \mathbf{q} momentum was obtained through $\hat{O}_{\mathbf{q}}^\dagger |\psi_0\rangle$ ($\hat{O}_{\mathbf{q}}^\dagger = \sum_j e^{i\mathbf{q} \cdot \mathbf{j}} c_j^\dagger$, with c_j^\dagger the hole creation operator at \mathbf{j} , dropping the spin index, in the rung basis). All states generated by this procedure were kept, and we worked in such a subspace in the subsequent iterations of the

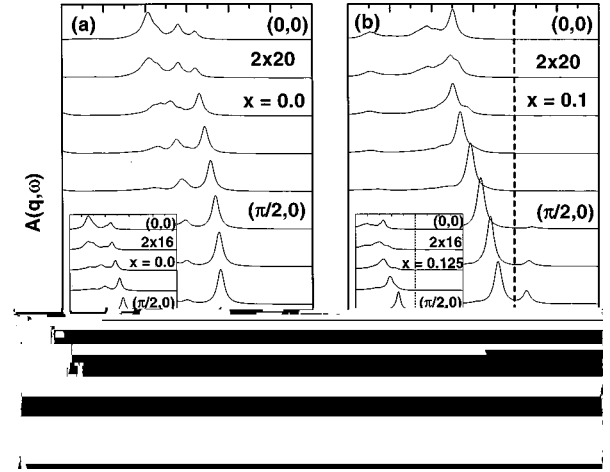


FIG. 2. $A(\mathbf{q}, \omega)$ for the bonding band $q_y=0$ on a 2×20 cluster. (a) corresponds to $x=0$ and (b) to $x=0.10$. The insets correspond to 2×16 clusters.

continued-fraction expansion.²³ Only the bonding band subspace is discussed here. The δ functions have a width 0.1t throughout the paper.

Figure 2(a) corresponds to the undoped limit. A sharp peak is observed at the top of the PES spectra, maximized at momenta $q_x=7\pi/10$, i.e., close to the Fermi momentum for noninteracting electrons $q_x^F=0.66\pi$. The band defined by those peaks has a small bandwidth, as in 2D models, due to the interaction of the injected holes with the spin background.^{23,24} Note that all peaks at momenta $q_x \geq \pi/2$ carry a similar weight and the dispersion is almost negligible. This unusual result is caused by strong correlation effects. The PES weight above q_x^F , e.g., at $q_x=\pi$, is induced by the finite but robust ξ_{AF} , and its existence resembles the antiferromagnetically induced ‘‘shadow’’ features discussed before in 2D models.²⁵

Figure 2(b) contains results at low but finite hole density. Several interesting details are observed: (i) the PES band near μ is flat. This should be an ARPES observable result resembling experiments in 2D cuprates, and it adds to the growing evidence linking the physics of ladders and planes; (ii) $q_x=\pi$ ($\pi/2$) PES has lost (gained) weight compared with $x=0$; (iii) the total PES bandwidth has increased; and (iv) the IPES band is intense near $q_x=\pi$, and it is separated from the PES band by a gap. The observed gap caused by hole pairing is $\Delta \sim 0.4t$. The DMRG/PBC binding energy calculated for the same cluster and density is $\sim 0.32t$ ($m=200$, truncation error $\sim 10^{-4}$). In the overall energy scale of the ARPES spectra, this difference is small and does not affect the study of the evolution of the dispersion shown here. Note that the results of Fig. 2(b) are similar to those observed near $(\pi,0)$ using ARPES for the 2D cuprates.^{9,15}

Figure 3(a) contains results at $x=0.1875$. The trends observed at $x=0.1$ continue, the more dramatic being the reduction of the $q_x=\pi$ PES weight caused by the decrease in ξ_{AF} . The lost weight appears in the $q_x=\pi$ IPES signal. The gap is still observed in the spectrum. Weak BCS-like features both in PES and IPES near q_x^F can be seen. Figure 3(b) contains data at $x=0.3125$, and up to 6×10^6 states. The Hilbert space is maximized at this density for the 2×16 cluster. Now the result resembles more a noninteracting system on a discrete lattice. The IPES signal is no longer very flat,

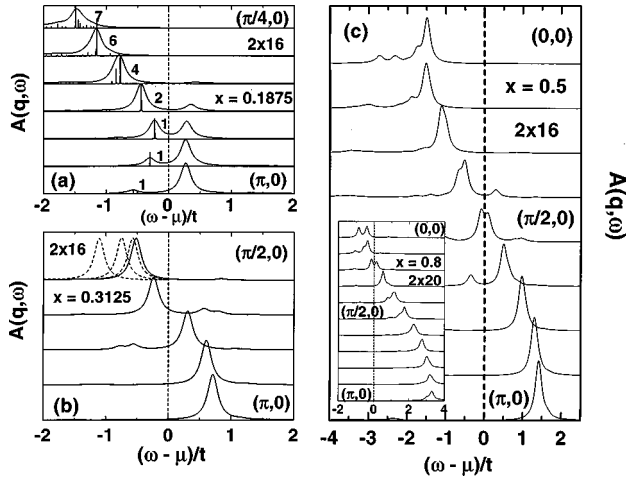


FIG. 3. Same as Fig. 2 but for a 2×16 cluster and the densities and momenta indicated. In (a) PES, results are also shown using a width $0.001t$ (and a different vertical scale) to visualize the δ functions. The number next to each broad peak is the number of poles contributing to it (some are difficult to resolve due to their small weight). In (b) and $\mathbf{q} = (\pi/2, 0)$ results obtained using 1.1, 2.8, 4.5 million states are shown (dashed lines) from left to right, to illustrate the convergence. The solid lines were obtained with 6.0 million states. At this density the basis space is maximized for the 2×16 cluster.

and the IPES band now has a clear energy minimum near the momentum where PES is maximized. Figure 3(c) contains results for $x = 0.5$ where a quasi-non-interacting dispersion is obtained using about 3×10^6 states in $|\psi_0\rangle$. The inset shows that the trend continues at lower electronic densities. The bandwidth evolves from being dominated by J near half-filling, to having t as a natural scale at $x \sim 0.3$ or larger. This evolution is smooth, yet *nontrivial*, following the reduction of ξ_{AF} with doping.

A conceptually interesting issue in the context of finite-cluster spectra of electronic models is whether finite line-widths for the dominant peaks can be obtained by such a procedure. Studying the small clusters reached by ED techniques it naively seems that those peaks are usually generated by just one δ function (one pole). However, in the bulk limit, peaks away from the Fermi level should have an intrinsic width. How can we reach such a limit from finite clusters? One possibility is that as the cluster grows, the number of poles N_p in a small energy window centered at the expected peak position must grow also, with their individual intensities becoming smaller such that the combined strength remains approximately constant. Consider as example Fig. 3(a) where the actual energy and intensity of the poles contributing to the main features are shown. As the peaks move away from the top of the PES band, N_p indeed increases providing evidence compatible with the conjecture made above.²⁶

Figure 4(a) contains the main-peak weights in the PES band vs density. Size effects are small. The weight at $q_x = \pi$ diminishes rapidly with x , following the strength of the spin correlations of Fig. 1(c). Overall the region affected the most by spin correlations is approximately $x \leq 0.25$. Figure 4(b) summarizes the main result of the paper, providing to the reader the evolution with x of the ladder dominant peaks

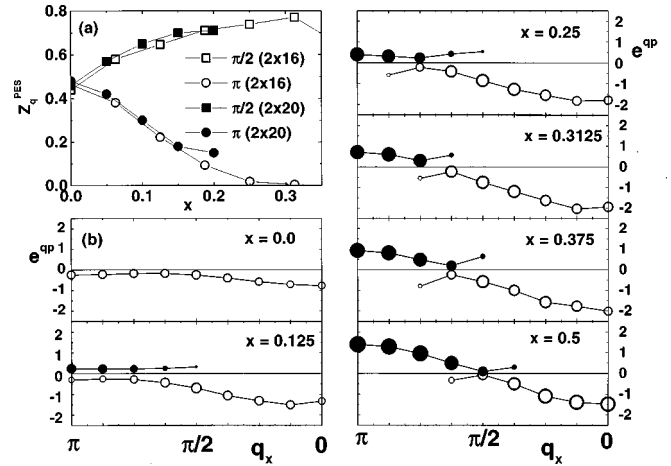


FIG. 4. (a) Weight of the low-energy dominant feature in $A(\mathbf{q}, \omega)$ for two momenta q_x in the bonding band vs x . Cluster sizes are indicated; (b) Evolution with doping of the dominant feature band ($t = 1$). The open (full) circles are centered at the peak energies e^{ap} below (above) μ . The hole densities are indicated. The area of the dots is proportional to the weight of the peak. The results can apply to 2D systems along the $(\pi, 0)$ - $(0, 0)$ line.

in $A(\mathbf{q}, \omega)$. The area of the circles are proportional to the peak intensities. At small x a hole-pairing-induced gap centered at μ is present in the spectrum, both the PES and IPES spectra are flat near $(\pi, 0)$, and the band is narrow. The PES flat regions at high momenta exist also in the undoped limit, where they are caused by the short-range spin correlations. Actually the undoped and lightly doped regimes are smoothly connected. As x grows to ~ 0.3 , the flat regions rapidly lose intensity near $(\pi, 0)$, and the gap collapses.

The many similarities between ladders and planes discussed in previous literature³ suggest that our results may also be of relevance for 2D systems along the line $(0, 0)$ - $(\pi, 0)$. For instance, the abnormally flat regions near $(\pi, 0)$ [Fig. 2(b)] are similar to ARPES experiments data for the 2D cuprates,⁹ and they should appear in high-resolution photoemission experiments for ladders as well. Note that in the regime studied with pairs in the ground state, the flat bands do not cross μ with doping but they simply melt. When x is between 0.3 and 0.4, a quasifree dispersion is recovered. The results of Fig. 4(b) resemble a Fermi-level crossing at $x \sim 0.3$ and beyond, while at small hole density no crossing is observed. It is remarkable that these same qualitative behaviors appeared in the ARPES results observed recently in underdoped and overdoped $\text{La}_{2-x}\text{Sr}_x\text{CuO}_4$.²⁷ These common trends on ladders and planes suggest that the large energy scale (LES) pseudogap (~ 0.2 eV) of the latter²⁸ may be caused by similar long-lived d -wave-like tight hole pairs in the normal state as it happens in doped ladders, where the pairing is caused by the spin-liquid RVB character of the ground state.³ In the 2D case a similar effect may originate in the finite ξ_{AF} observed in the underdoped finite temperature regime (although there is no evidence in the 2D materials of a spin liquid). A consequence of this idea is that the pairs and LES ARPES pseudogap are correlated and they should exist if ξ_{AF} is non-negligible,²⁹ a prediction that can be tested experimentally.

Summarizing, the spectral function of the two-leg t - J model has been calculated, and results can be used to guide future ARPES experiments for ladder compounds. These experiments should observe flat bands and gap features near $(\pi, 0)$ in the normal state. The data were found to be remarkably similar to results for the 2D cuprates along the $(0, 0)$ - $(\pi, 0)$ line. A common explanation for these features was proposed. In addition, note that the ORBA method dis-

cussed here introduces a way to calculate dynamical properties of spin and hole models on intermediate size clusters. The method can be applied to a variety of strongly correlated electronic models.

The authors specially thank J. Riera for many useful suggestions. Support from the NSF (DMR-9520776), CNPq-Brazil, CONICET-Argentina, and the NHMFL In-House Research Program (DMR-9527035) is acknowledged.

-
- ¹B. Levy, *Phys. Today* **49** (10), 17 (1996).
²M. Uehara *et al.*, *J. Phys. Soc. Jpn.* **65**, 2764 (1996).
³E. Dagotto and T. M. Rice, *Science* **271**, 618 (1996).
⁴T. Takahashi *et al.*, *Phys. Rev. B* **56**, 7870 (1997); T. Sato *et al.*, *J. Phys. Chem. Solids* (to be published).
⁵T. Mizokawa *et al.*, *Phys. Rev. B* **55**, R13 373 (1997).
⁶T. Mizokawa *et al.* (unpublished).
⁷Z.-X. Shen and D. S. Dessau, *Phys. Rep.* **253**, 1 (1995).
⁸D. S. Marshall *et al.*, *Phys. Rev. Lett.* **76**, 4841 (1996).
⁹D. S. Dessau *et al.*, *Phys. Rev. Lett.* **71**, 2781 (1993).
¹⁰H. Tsunetsugu *et al.*, *Phys. Rev. B* **49**, 16 078 (1994); M. Troyer *et al.*, *ibid.* **53**, 251 (1996); R. Eder *ibid.* **57**, 12 832 (1998).
¹¹S. Haas and E. Dagotto, *Phys. Rev. B* **54**, R3718 (1996).
¹²J. Riera, D. Poilblanc, and E. Dagotto, *Eur. Phys. J. B* **7**, 53 (1999).
¹³H. Endres *et al.*, *Phys. Rev. B* **53**, 5530 (1996).
¹⁴H. Endres *et al.*, *Physica B* **230-232**, 811 (1997); see, also, R. Noack *et al.*, *Phys. Rev. B* **56**, 7162 (1997).
¹⁵A. Loesser *et al.*, *Science* **273**, 325 (1996); H. Ding *et al.*, *Nature (London)* **382**, 51 (1996).
¹⁶J. Riera and E. Dagotto, *Phys. Rev. B* **47**, 15 346 (1993); **48**, 9515 (1993), and references therein.
¹⁷See E. Dagotto *et al.*, *Phys. Rev. B* **58**, 12 063 (1998).
¹⁸S. R. White, *Phys. Rev. Lett.* **69**, 2863 (1992). Some studies of dynamical properties using the DMRG technique are in K. Hallberg, *Phys. Rev. B* **52**, R9827 (1995).
¹⁹For the 2×16 cluster, the Hilbert space is maximized for 10 holes reaching $\sim 10^{12}$ states. In this situation e_{GS} was 0.76 with ORBA, and 0.768 with the DMRG method ($m=200$) using this time-periodic boundary conditions (PBC) in both cases. The error is in the last digit.
²⁰For densities $0.2 \leq x \leq 0.5$, where the size of the Hilbert space is the largest, the convergence on the 2×20 cluster was not good enough for our purposes.
²¹C. Hayward and D. Poilblanc, *Phys. Rev. B* **53**, 11 721 (1996).
²²The shapes of the spectral functions are very similar irrespective of whether a small fraction of $|\psi_0\rangle$ is used or the full state. They differ only in an energy shift. Thus, most of the *qualitative* features of the ARPES spectra can be obtained with only a fraction of the states used here.
²³E. Dagotto, *Rev. Mod. Phys.* **66**, 763 (1994).
²⁴The ARPES peaks in the 2D cuprates for some momenta and densities are broad and they cannot be labeled as quasiparticles.
²⁵S. Haas *et al.*, *Phys. Rev. Lett.* **74**, 4281 (1995).
²⁶For the importance of calculations incorporating line shapes see M. Norman *et al.*, cond-mat/9711232 (unpublished).
²⁷A. Ino *et al.*, cond-mat/9809311 (unpublished); see also A. Ino *et al.*, *Phys. Rev. Lett.* **81**, 2124 (1998).
²⁸P. J. White *et al.*, *Phys. Rev. B* **54**, R15 669 (1996).
²⁹Thus, in this context the preformed pair [C. Sa de Melo *et al.*, *Phys. Rev. Lett.* **71**, 3202 (1993)], and magnetic [A. Chubukov *et al.*, *J. Phys.: Condens. Matter* **8**, 10 017 (1996)] scenarios are mixed together.